International Journal of Heat and Mass Transfer 51 (2008) 5712–5720

Contents lists available at ScienceDirect

International Journal of Heat and Mass Transfer

journal homepage: www.elsevier.com/locate/ijhmt

Plasma microcirculation in alveolar capillaries: Effect of parachute-shaped red cells on gas exchange

A.A. Merrikh [a], J.L. Lage [b,*]

[a] Advanced Micro Devices, AMD, 5204 E. Ben White Blvd MS 523, Austin, TX 78741, United States
[b] Laboratory for Porous Materials Applications, Department of Mechanical Engineering, Southern Methodist University, Dallas, TX 75275-0337, United States

ARTICLE INFO

Article history:
Received 20 February 2008
Received in revised form 4 April 2008
Available online 12 June 2008

Keywords:
Alveolus
Gas exchange
Capillary
Blood flow

ABSTRACT

The effects of plasma microcirculation speed and red blood cell (RBC) shape on CO exchange in alveolar capillaries is numerically investigated. In this study, blood is modeled as an inhomogeneous, two-constituent substance, with one of the constituents being the blood plasma, treated as a homogeneous Newtonian fluid, and the other being the RBCs, treated as discrete, suspended particles (i.e., solid bodies) flowing with the plasma. The RBC shape and blood speed effects on the alveolar diffusion process is observed not only by the variations in the iso-lines along the alveolar capillary but also by changes in the lung diffusing capacity. The simulations include varying the capillary blood speed from 1.0 to 10 mm/s and the capillary hematocrit from 3% to 55%. The RBC shape effect is established by comparing results obtained for circular RBCs to results for which the RBCs have a more realistic, parachute shape when flowing with the plasma. Results reveal the parachute-shaped RBCs yield higher lung diffusing capacity compared to the circular ones. Moreover, blood flow can increase the lung diffusing capacity by almost 50% in certain cases, with the effect being more predominant at high blood speed and low hematocrit. Finally, the effect of blood speed for parachute-shaped RBCs is quantified in terms of percentage-increase lung diffusing capacity and presented in a simple predictive equation.

1. Introduction

The understanding of gas transport in alveolar capillaries is not only helpful for diagnostics of lung diseases, but also important in the design of next-generation oxygenators and artificial lungs. In addition, due to the analogy between heat and mass transfer, much of what is learned on gas (mass) transport in lung capillaries can be applied, in principle, to heat transfer in microchannels, an area of importance to such practical applications as cooling of microelectronics and MEMS.

Alveolar capillary blood is separated from the alveolar gas region by a sheet barrier. This sheet, which delimits the alveolar sack, is the structural components of the alveolus, giving to it a honeycomb-like appearance (Fig. 1a). These sheets, made of the alveolar and capillary membranes sandwiching interstitial fluid, is what forms the alveolar capillary. In general, the alveolar capillary allows for only a single layer of RBCs to flow through. Inhaled diffusive gases (CO, O_2, NO, etc.), have to pass through this sheet to reach the blood flowing through the capillaries; diffusing gases leaving the body have also to pass through the same sheet to reach the alveolar gas region. A close-up section of a dog's single lung capillary is visible in Fig. 1b.

Despite the geometrical complexity of the alveolar capillary region and the large number of participating constituents, simplified theoretical models remain essential for improving the understanding of the gas exchange process, including the effects of the transport parameters on the gas exchange, and for establishing the correct form–function relationships ruling the alveolar gas exchange.

The original work of Krogh and Krogh [1] recommended the lung diffusing capacity DL as a measure of the lung efficiency in transferring gas to the capillary blood, where

$$\mathrm{DL} = \frac{\dot{V}}{(P_A - P_{RBC})} \tag{1}$$

with $\dot{V}$ being the volumetric rate of gas uptake by the blood, and P_A and P_{RBC} being, respectively, the gas partial pressure in the alveolar gas region and in the RBC. These two partial pressures, by the way, represent the two concentrations believed to drive the gas transfer process. Analogous to a direct current electric circuit, Eq. (1) predicts the current $\dot{V}$ driven by the single potential difference $(P_A - P_{RBC})$ across the resistance (1/DL). Therefore, the resistive effects of all of the constituents of the alveolar region are lumped into a single parameter in Eq. (1), namely the resistance (1/DL).

The lung diffusing capacity DL can be estimated from relatively simple measurements following existing protocols, such as the single breath [2] or the re-breathing [3] techniques. Typically, CO is

* Corresponding author.
E-mail address: jll@engr.smu.edu (J.L. Lage).

0017-9310/$ - see front matter © 2008 Elsevier Ltd. All rights reserved.
doi:10.1016/j.ijheatmasstransfer.2008.04.016

Nomenclature

d	gap size between an RBC and the capillary membrane
D	gas diffusivity, $\mu m^2/s$
DL	lung diffusing capacity, m^3/s Torr
H	capillary thickness, μm
H_t	membrane thickness, μm
Ht	hematocrit
L	length, μm
N_{RBC}	number of RBCs inside the capillary
p	capillary pressure, mmHg
P	gas partial pressure, Torr
t	time, s
U	RBC speed, mm/s
u, v	velocity components, mm/s
$\mathbf{v}$	velocity vector
x, y	Cartesian coordinates, μm
V	volume, μm^3
$\dot{V}$	volumetric gas uptake, $\mu m^3/s$
$\dot{V}''$	gas flux, $\mu m/s$

Greek symbols

α, β	curve fitting constants
α_{CO}	Bunsen solubility coefficient, $Torr^{-1}$
ε	percent increase lung diffusing capacity
θ	specific rate of gas uptake, $\mu m^3/s$ Torr RBC
μ	dynamic viscosity, s Pa
τ	single breath-hold time, s

Subscripts

A	alveolar gas
B	barometric
c	convection
d	diffusion
CO	carbon monoxide
CO-p	CO property in plasma
CO-m	CO property in membrane (tissue)
m	membrane
p	plasma
RBC	red blood cell

preferred for testing the lung diffusing capacity because of the tremendous affinity it has for hemoglobin, allowing for the simplifying approximation $P_{RBC} = 0$ in Eq. (1).

A more elaborate analytical representation of DL can be obtained following a lumped capacity approach consistent with Krogh's original idea. The result, basis for the widely used single breath technique for obtaining DL, is the Krogh equation [4,5]:

$$DL = \frac{V_A}{(P_B - 47)\tau} \ln\left(\frac{P_{A-0}}{P_{A-\tau}}\right) \tag{2}$$

where V_A is the alveolar gas volume, P_B is the barometric pressure, τ is the single breath-hold time, and P_{A-0} and $P_{A-\tau}$ are the alveolar CO partial pressures at $t = 0$ (inhaling time) and at $t = \tau$ (exhaling time), respectively. In Eq. (2), the effects of all of the components of the alveolar respiration are lumped into only two parameters, namely V_A and $P_{A-\tau}$ (note that τ is set for the test, and P_{A-0}, the inhaling partial pressure of CO, also has a prescribed known value).

Eqs. (1) and (2) allow the physical interpretation of DL as a measure of the lumped capacity of the lungs to transfer gas to the blood. Hence, DL can be seen as a system-level performance parameter. As such, changes in DL imply changes in the performance of the entire system. The need for linking the changes in DL to changes in the components of the system (e.g., alveolar gas region volume, capillary membrane thickness and blood volume, hematocrit or hemoglobin concentration, capillary topology, blood speed, and RBC shape) is fundamental for better understanding the respiration process and, by consequence, for improving diagnoses based on changes in DL.

Roughton and Forster [6] proposed a simplified analytical model linking the total resistance to gas uptake (1/DL), to the representative membrane diffusing resistance (1/DM) and the RBC diffusing resistance ($1/(\theta V_C)$) leading to

$$\frac{1}{DL} = \frac{1}{DM} + \frac{1}{\theta V_C} \tag{3}$$

where θ is the specific rate of gas uptake by the blood and V_C is the pulmonary capillary blood volume. Johnson et al. [7] presented an equation for determining θ as a function of the alveolar O_2 tension (P_{A-O_2}), which is very useful when studying CO diffusion. Hence, Eq. (3) allows the prediction of DM and V_C from independent physiolog-

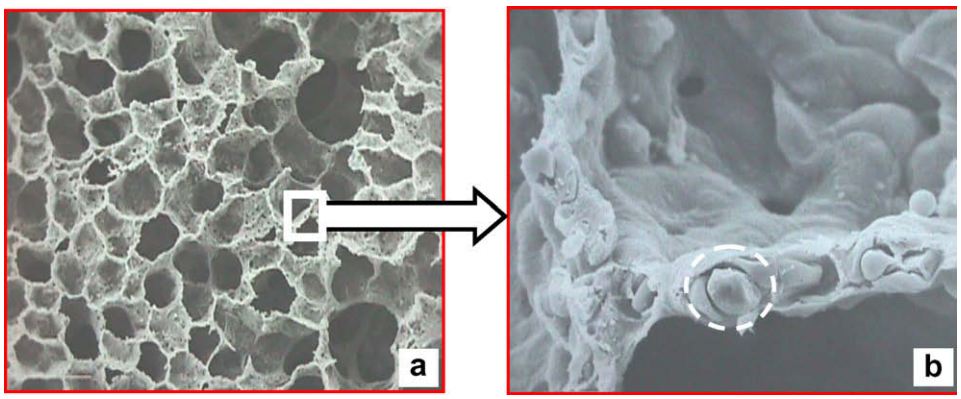

Fig. 1. Scanning electron micrograph of a dog lung showing (a) the complex internal overall structure of the alveolar region and (b) a close-up of the capillary bed showing a red blood cell within the dashed circle. (Courtesy of Prof. C.C.W. Hsia, UT-SW Medical Center, Dallas, TX.)

ical measurements of DL (via single-breath technique, Eq. (2), for instance) at two different P_{A-O_2} values. This procedure is known as the RF-method.

The morphometric (M) method [8] emerged as an alternative to the RF-method to linking DL to local parameters believed to influence the alveolar respiration. The M-method uses Eq. (3) to predict DL from estimates of DM and V_C obtained from a fixed lung following stereological principles. Observe that the RF-method and the M-method require previous knowledge of θ.

More importantly in Eq. (3) is, perhaps, the lumping of the effects of all components of the alveolar respiration into only three parameters, DM, V_C, and θ. Moreover, by analogy to a direct-current electric circuit and in conjunction with Eq. (1), Eq. (3) represents the equivalence of two resistances in series (i.e., the membrane and RBC resistances), on the pathway of the current (gas flux) driven by single values of a high and a low potential (gas partial pressures), a simplified view of the actual process taking place in a pulmonary capillary. Observe in Eq. (3) the absence of specific terms accounting for the transient and convective effects of the blood flow. These terms, and other effects, are hidden (or lumped) in the measured parameters involved in Eqs. (1)–(3).

An alternative to unveil the effects played by each component of the alveolar system is to simulate the local gas diffusion process numerically. This alternative is equivalent to enhancing the visual resolution of the alveolus (from the lumped approach of the Krogh model or the resistances-in-series approach of the RF-method), allowing for the examination of individual components. However, the higher visual definition needed for simulating the process at the component level leads to increased difficulty because of the different length scales involved and the complex geometry of the alveolar region. Therefore, most numerical studies use simplified models of the alveolar region, as described subsequently. Moreover, some studies of gas exchange in muscle capillaries are of importance because the process of gas transport by the blood is very similar in both cases. Hence, they are also included.

More than 35 years ago, Aroesty and Gross [9] published a paper on steady-state gas diffusion inside a straight capillary, between muscle tissue and flowing blood. Their main conclusion was that, in muscle capillaries, blood velocity does not affect the gas transport between surrounding tissue and RBCs, leading to the neglect of the convective terms of the gas transport equations by many researchers who studied gas transport process either in muscle capillaries or in pulmonary capillaries.

For a heat and mass transfer specialist, the conclusion reached by Aroesty and Gross [9] would certainly attract careful scrutiny because it is well known that transport processes are enhanced when flow (or convection) is present. It so happens that the transport configuration considered by Aroesty and Gross [9], when seen from a mass transfer perspective, would help justify their conclusion. For instance, the modeling of the red cells as long cylinders aligned with the blood flow direction, with the surface in contact with the surrounding tissue, provides an easy path for transport from the tissue directly to the RBCs via diffusion. Another aspect, a consequence of the same geometrical configuration, is the circulation generated in the plasma region. It is easy to conclude that this circulation enhances the gas transport process along one of the RBC surfaces bathed by the plasma, but in fact it hinders the transport along the opposite surface, canceling the convective effect. These aspects have been recently discussed in more detail by Merrikh and Lage [10–12].

It is possible to ascertain that the conclusion in Aroesty and Gross [9] is based mainly on geometrical and physiological factors, which can be questioned as too simplistic, unrealistic, or not broad enough to be applied to the transport phenomena happening in capillaries. For instance, some important factors not considered are the RBC shape (parachute-like instead of cylindrical), the shape of the lung capillary bed (a sheet-like configuration as opposed to a circular tube), and the discrete nature of the RCBs. Another important factor directly related to the blood flow has to do with the role played by the plasma. As blood flows inside the capillary, the resistance provided by the surrounding capillary tissue forces the plasma, trapped within consecutive RBCs, to circulate. Although the contribution of this circulation (convection) effect could indeed be negligible for certain parametric ranges, the blood flow, nevertheless, replenishes the capillary region with fresh plasma as it flows through the capillary. This replenishment, not accounted for by Aroesty and Gross [9] and later research, certainly impacts the gas transport. When properly considered, each one of these factors can affect the blood convective effect on the gas diffusion process, potentially altering the conclusion reached by Aroesty and Gross [9], that of blood convection playing no role in the alveolar diffusion process.

The study of inhomogeneous (two-phase) blood in capillaries by Hellums [13] is of interest for also treating blood as an inhomogeneous fluid, with plasma (liquid) and RBC (solid) modeled separately as distinct constituents. In this case, the gas transport was considered through RBCs only, with the effect of plasma being neglected. Later on, Federspiel and Popel [14] studied oxygen unloading of RBCs in muscle capillaries including the plasma, but convection effects were again neglected. Their main conclusion was that RBCs compete for oxygen, as indicated by the decay in the gas concentration gradient close to the capillary centerline in between consecutive RBCs, leading to a lower amount of oxygen uptake *per RBC* at high hematocrit. However, they emphasized that, although the total oxygen release per RBC decreases by diffusion interaction between the erythrocytes at high hematocrit, it increases per unit tissue area with the decreasing distance between consecutive RBCs. Federspiel [15] investigated pulmonary oxygen transport for stationary RBCs in single-file suspension flowing through a straight, two-dimensional pulmonary capillary. Blood flow effects were neglected. He found that increasing the membrane thickness decreases the amount of gas transferred to the RBCs.

Groebe and Thews [16] analyzed oxygen release in maximally working skeletal muscle for a blood velocity of up to 4 mm/s. They found that RBC movement can lead to a 20% increase in the overall capillary oxygen release. They focused on the effect of plasma gaps on the oxygen release process. In their model, overall (surface averaged) oxygen release rate fluctuated because of the plasma gaps and the frequency of oscillations increased with a decreasing gap between the RBCs, an expected phenomenon. The shape of RBCs in their analysis, however, was cylindrical, with no gap between RBCs and muscle tissue, limiting the convective transport to the flow ensuing in the gap between RBCs, similar to the configuration studied by Aroesty and Gross [9].

The effect of parachute-shaped RBCs in muscle capillaries seems to have been studied first by Wang and Popel [17]. In their numerical investigation, a straight, two-dimensional muscle capillary was filled with parachute-shaped entities in a single-file suspension, for a capillary hematocrit of 26%. In their model, the convective terms pertinent to the transport of partial pressure of oxygen in plasma were neglected, again subscribing to the main conclusion by Aroesty and Gross [9]. They pointed to the importance of RBC shape and its impact on gas exchange, concluding that RBC shape has a significant influence on the overall amount of diffusive gas exchange in capillaries.

Hsia et al. [18] studied the differences between their finite element model predictions and the RF-method and M-method predictions. They found the RF-method accurately predicted DL_{CO} at low hematocrit but over-predicted it at high capillary hematocrit. They also examined two different values of θ_{CO}, and found that higher oxygen tension of the alveolar gas decreases the rate of

CO transport into the capillary, as expected. In Hsia et al. [19], the differences between DL_{CO} parachute-shaped RBCs and circular shaped RBCs were studied. They found that circular RBCs in a straight, two-dimensional capillary result in a higher lung diffusing capacity compared to the lung diffusing capacity for parachute-shaped RBCs. The difference was attributed to the higher diffusion path associated with the parachute-shaped RBCs. Subsequently, Frank et al. [20] studied the effect of parachute-shaped RBCs, in two-dimensional and axisymmetric configurations, for oxygen transport in pulmonary capillaries. They found that both models, either two-dimensional or axisymmetric, highly over-predict the experimental measurements of membrane diffusing capacity, because of the exaggerated membrane–plasma surface of cylindrical capillary assumption. All these studies considered diffusion only, with the RBCs stationary inside a capillary.

Bos et al. [21] questioned the work by Aroesty and Gross [9]. Considering cylindrical capillary, cylindrical RBCs and no gap between RBCs and tissue, they argued that convection can be significant, but not as a result of the configuration, but as a result of the boundary conditions imposed by Aroesty and Gross [9] at the surfaces of the capillary. Varying the boundary condition within the convective region, as well as along the surface of the RBC, they concluded that convection within the gap between RBCs can be important for the same velocity range considered by Aroesty and Gross [9].

Among the few who included blood movement in the model, Patel [22] modeled an annular solid, representing the RBCs, moving in the middle of a two-dimensional capillary, the properties of which were changed with time to represent movement of blood and plasma gaps. The author reported that the blood movement had no significant effect on the rate of oxygen transport, and that the only effect responsible for the increase in oxygen transport during exercise is the increase in the capillary blood volume. No details were revealed on the hydrodynamics of the capillary microcirculation and on why the blood flow effects were unimportant.

2. Formulation

In the quest to investigate in greater detail the effects of blood flow in alveolar capillary, the present investigation gives specific attention to the morphology of the RBCs, hoping to identify its effects on the CO transport in a pulmonary capillary. The domain of interest is depicted in Fig. 2, showing a straight capillary through which plasma and RBCs flow from left to right. The capillary surface, called "tissue", in fact represents the two membranes separating the blood from the gas region of the alveolus. Hence, the lower surface of the tissue region would play the role of the capillary membrane, and the upper surface would be the alveolar membrane. The RBCs, considered solid particles, have a parachute-like shape, move with a uniform speed and are separated by a uniform distance from one another and from the capillary membrane surface.

Assuming the blood plasma as homogeneous, incompressible, and Newtonian, with constant physical properties, the model equations for plasma hydrodynamics in the capillary are the continuity and momentum equations, respectively:

$$\nabla \cdot \mathbf{v} = 0 \tag{4}$$

$$\rho_p \left[\frac{\partial \mathbf{v}}{\partial t} + (\mathbf{v}\cdot\nabla)\mathbf{v}\right] = -\nabla p + \mu_p \nabla^2 \mathbf{v} \tag{5}$$

where $\mathbf{v}$ is the velocity of the plasma with components (u,v) in the x- and y-directions, respectively, ρ_p and μ_p are the plasma density, assumed equal to 1.035 g/ml, and viscosity, assumed equal to 0.012 P, respectively. The model equations for gas diffusion in the membrane and plasma regions, respectively, can be written in terms of CO partial pressure, P, as [12,18]

$$\frac{\partial P}{\partial t} = D_{\text{CO-m}} \nabla^2 P \tag{6}$$

$$\frac{\partial P}{\partial t} + \mathbf{v}\cdot\nabla P = D_{\text{CO-p}} \nabla^2 P \tag{7}$$

where $D_{\text{CO-m}}$ and $D_{\text{CO-p}}$ are the diffusion coefficients of CO in the membrane and plasma regions, respectively, both being set as equal to 2.45×10^3 μm^2/s. Conservation of CO partial pressure and gas flow rate along the interface ($y = H$) of capillary membrane (tissue) and blood plasma leads to the following compatibility conditions:

$$P_m|_{y=H} = P_p|_{y=H} \tag{8}$$

$$D_{\text{CO-m}} \left.\frac{\partial P_m}{\partial y}\right|_{y=H} = D_{\text{CO-p}} \left.\frac{\partial P_p}{\partial y}\right|_{y=H} \tag{9}$$

Due to the much higher CO diffusivity, and as discussed by Hsia et al. [18], the alveolar air space is assumed to be an infinite reservoir of CO. Thus, the CO partial pressure along the upper boundary of the tissue region is set as uniform and constant, equal to 1 Torr ($P_{\text{CO-m}}|_{y=H+H_t} = 1$ Torr).

As discussed by Merrikh and Lage [12], the RBCs can be considered infinite sinks for CO; so, the internal boundary condition of constant CO partial pressure can be set inside the RBCs, namely

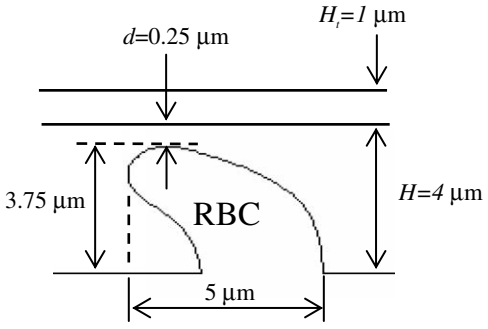

Fig. 3. Red blood cell and tissue relative dimensions (adapted from [19]; original from scanning electron micrograph of [23].)

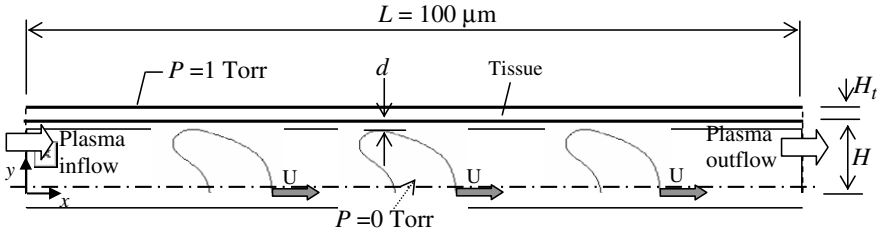

Fig. 2. Sketch of the capillary domain showing blood flowing with three RBCs.

Table 1
Dimensions and property values used in the simulations

Parameter	Value
L	100 μm
H	4 μm
H_t	1 μm
$D_{CO\text{-}p}$	2.45×10^3 μm^2/s
$D_{CO\text{-}m}$	2.45×10^3 μm^2/s
P_{RBC}	0.0 Torr
ρ_p	1.035 g/ml
μ_p	1.2 cP

$P_{CO\text{-}RBC} = 0$. The RBC resistance to CO uptake, including the reaction with hemoglobin, $1/\theta_{CO}$, is modeled as a resistance across a thin red cell membrane; this resistance is varied in accordance with the assumed alveolar oxygen tension (in mmHg) to accurately mimic the values of θ_{CO}. The local amount of CO flux crossing the membrane (equivalent to the CO uptake by the blood) is obtained from

Table 2
Element grid side-lengths for Fig. 4

Level	Tissue (μm)	Plasma (μm)	RBC surface (μm)	DL_{CO} (μm/s Torr)
I	0.5	0.5	0.2	**0.891**
II	0.25	0.25	0.1	**0.886**
III	0.15	0.15	0.075	**0.885**

Grid-independent results for $U = 10$ mm/s and Ht = 3.09%. DL_{CO} results obtained for $\theta_{CO} \to \infty$.

$$\dot{V}'' = -\alpha_{CO} D_{CO\text{-}p} \left.\frac{\partial P}{\partial y}\right|_{y=H} \tag{10}$$

where α_{CO} is the Bunsen solubility (or Henry) coefficient, equal to 2.36×10^{-5} Torr^{-1} for the case of CO dissolved in water. The total CO volumetric flow rate can be obtained by integrating the flux along the membrane–plasma interface:

$$\dot{V} = \int_{A_m} \dot{V}'' \, dA \tag{11}$$

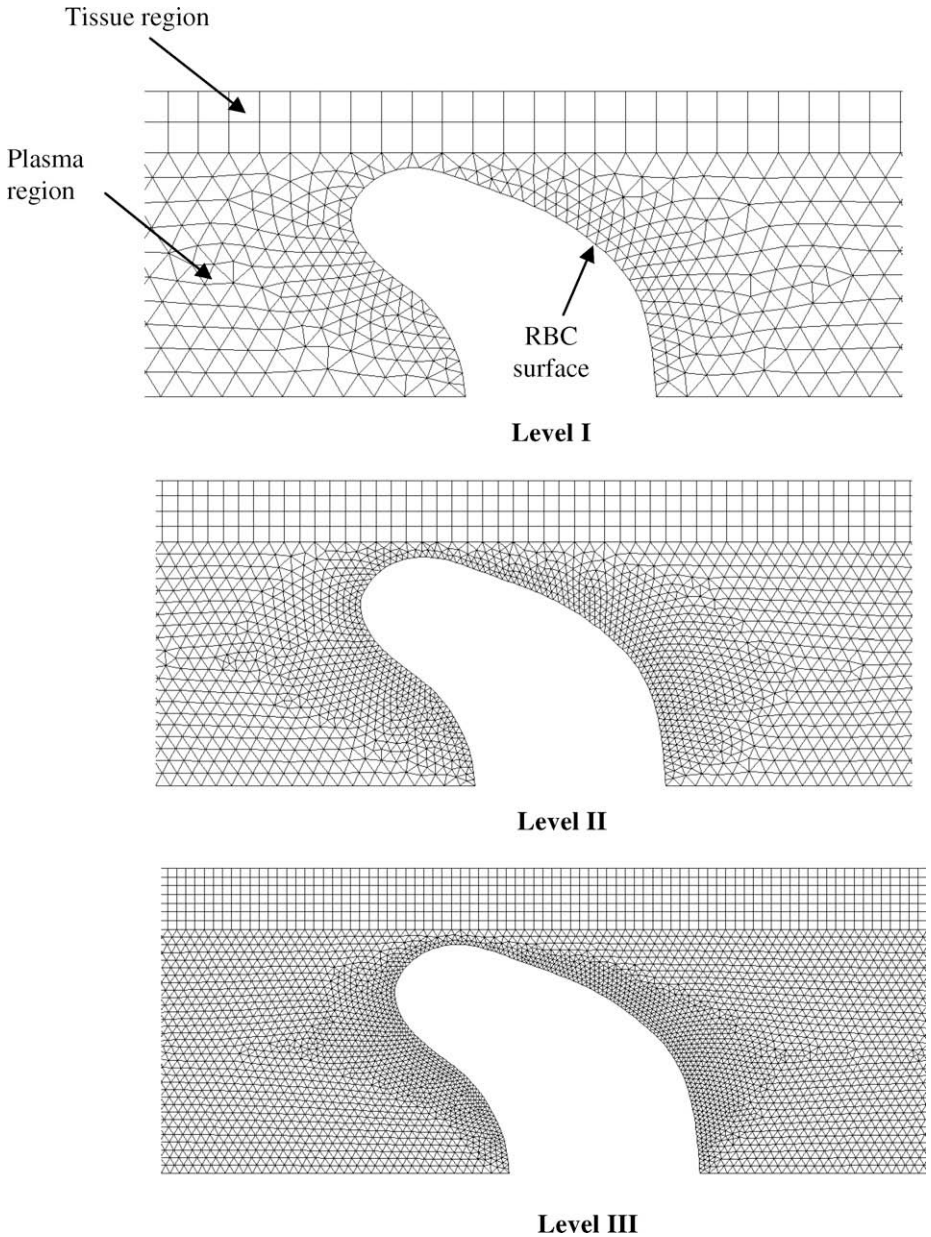

Fig. 4. Example mesh levels for studying grid effect on the numerical simulation results (refer to Table 2 for details).

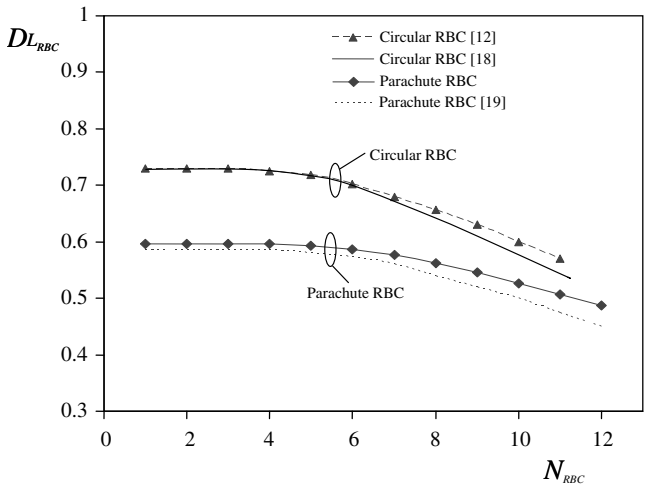

Fig. 5. Comparison of pure diffusion results for circular and parachute-shaped RBCs (results for $\theta_{CO} \to \infty$).

where A_m is the surface area of the capillary membrane through which CO is transferred into the capillary blood (in this case 100 μm^2) and $\dot{V}''$ is the flux of CO crossing the membrane–plasma interface, defined via Eq. (10). With the result from Eq. (11), the lung diffusing capacity, as defined by Krogh and Krogh [1], can be calculated from Eq. (1) for CO. Another important parameter worthy of mention is the lung diffusing capacity per RBC, defined as

$$DL_{RBC} = \frac{DL_{CO}}{N_{RBC}} \tag{12}$$

where N_{RBC} is the number of RBCs occupying the capillary length in which gas exchange takes place.

3. Results and discussion

3.1. Numerical solution

The shape of the RBCs is realistically adapted from an originally digitized RBC scanning electron microscopy of Skalak and Branemark [23], also adopted by Hsia et al. [19], fitted with cubic splines

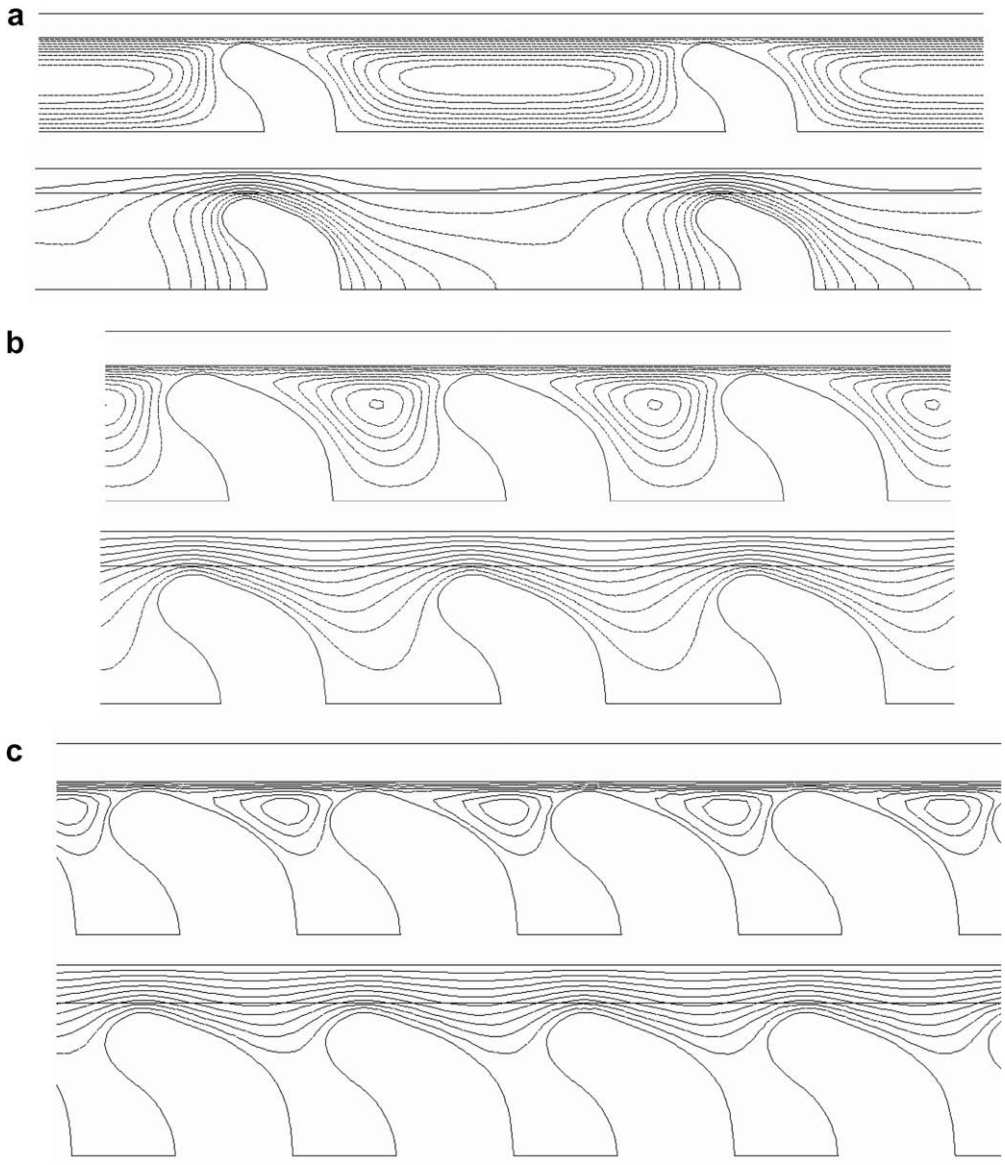

Fig. 6. Streamlines (top) and isobaric lines (bottom) with $U = 10$ mm/s for (a) 5 RBCs (Ht = 15.52%), (b) 12 RBCs (Ht = 37.28%), and (c) 17 RBCs (Ht = 52.82%).

as a cross-section of the RBC, Fig. 3. The model equations presented in the previous section were numerically solved by the finite-volume method with the QUICK scheme. For faster convergence, a multi-grid technique was used. Rectangular-shaped elements in the tissue region and triangular-shaped elements (unstructured grid) in the plasma region were used to better accommodate the parachute-shaped RBC surface. A summary of all the parameters, constants and dimensions used in this study is presented in Table 1.

Grid independence of the numerical scheme was verified by comparing the solutions obtained from the most stringent case considered here, namely the highest blood velocity, $U = 10$ mm/s, and lowest hematocrit, i.e., a single RBC flowing through the channel (as already shown in [12], for the case of circular RBCs, the lowest hematocrit configuration yields the strongest convective effect inside the capillary, or in other words the steepest velocity gradients). Three different grids were used, as shown in Fig. 4, named Level I, Level II, and Level III grids. The grid distribution was varied by decreasing the element side lengths in each region. For the tissue region, the surface mesh was varied directly; for the plasma region, first the RBC surface was meshed, leading to an "adaptation" of the plasma mesh to the RBC according to its highest side length presented in Table 2. The grid independence test results shown in Table 2 revealed that the Level II grid was sufficient as the difference between Level II and Level III grids was less than 1%. It is also worth mentioning that for the pure diffusion case (zero blood speed), the results from all three grid levels are in perfect agreement.

The mathematical formulation and the numerical solution procedure followed here were validated further through a comparison of the DL_{RBC} values available in the literature, obtained for the case of two-dimensional, steady-state, diffusion with zero blood flow (stationary blood). For a wide hematocrit (Ht) range, and for θ_{CO} equal to infinity (equivalent to no RBC resistance to gas flow), the results were compared to the results obtained by Hsia et al. [19] for the parachute-shaped RBC case, as shown in Fig. 5. Considering the difference between the two numerical approaches (Hsia et al. [19] used the finite-element method and different element sizes), the results compare well. The maximum discrepancy of 9% observed between the results for high hematocrit (for $N_{RBC} > 6$), can be attributed to the numerical scheme used by Hsia et al. [19] (it is unclear if their results are grid independent). Included in the figure are results obtained for circular RBCs, obtained by Merrikh and Lage [12] and by Hsia et al. [18], to show that a similar trend in the discrepancy of the results obtained from the finite-volume and finite-element schemes is observed in this case as well for high hematocrit.

3.2. Effect of hematocrit on DL_{CO} variation

Now, the effects of hematocrit and blood speed on the diffusion process are presented. Fig. 6 shows first the patterns of streamlines (above) and isobaric lines (equivalent to iso-concentration lines, below) for blood speed equal to 10 mm/s, and three different hematocrit levels, namely 15.52% (Fig. 6a), 37.28% (Fig. 6b) and 52.82% (Fig. 6c).

Observe that increasing the hematocrit is equivalent to reducing the distance between successive RBCs as they flow through the capillary. Interestingly, looking at the streamline patterns of Fig. 6 from top to bottom (from Fig. 6a–c), a reduction in the circulation strength in the plasma region between the RBCs is observed. As the RBCs get closer to each other, the viscous resistance of their surfaces and of the capillary membrane hinders the circulation flow, restricting it to a region very close to the tissue surface. This aspect supports the comment made in relation to the grid independence tests.

For low hematocrit (less number of RBCs in the capillary) the isobaric line pattern of Fig. 6a shows a minimal interference between RBCs because the distance between them is large enough for their competing effect for CO coming from the capillary mem-

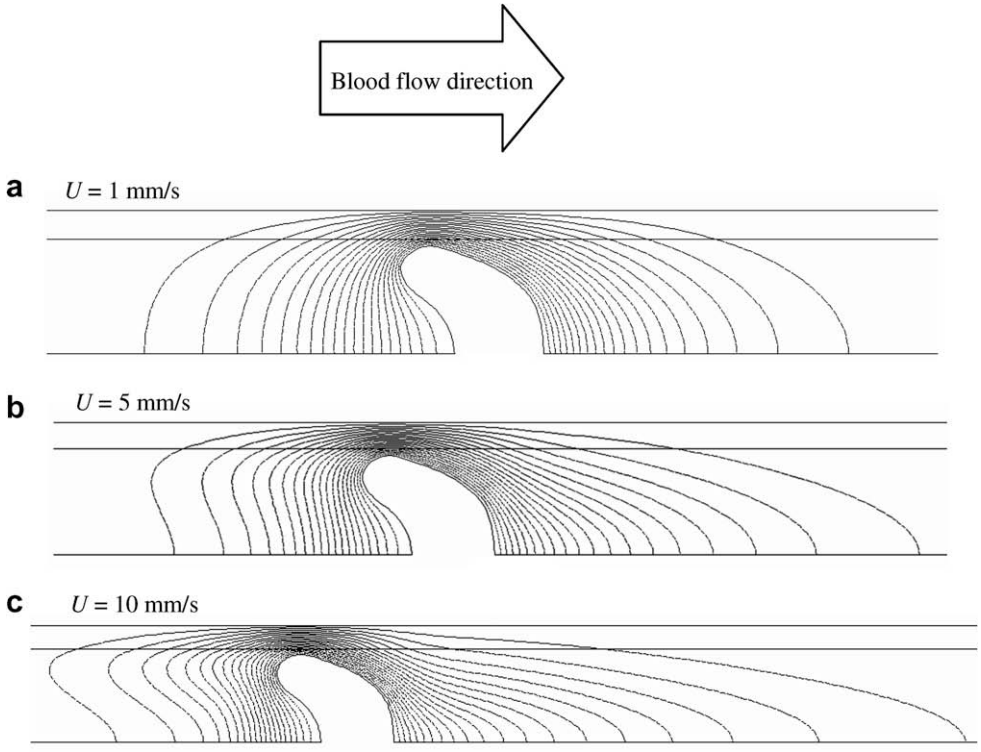

Fig. 7. Isobaric lines for a single RBC (Ht = 3.09%) flowing in the capillary with (a) $U = 1$ mm/s, (b) $U = 5$ mm/s and (c) $U = 10$ mm/s.

brane to be small. However, as the RBCs get closer to each other, the competition between them for receiving CO eventually leads to a reduced concentration field in between them, as seen in Fig. 6b and c. This, in turn, results in a decrease in the gas transfer rate to the lower part of the RBC surface (close to the center line of the capillary), which in turn results in a drop in the global gas transfer rate to the RBCs. Similar observations were also reported by Merrikh and Lage [12] for the case of circular RBCs.

In Fig. 7, the effect of increasing the blood speed is shown depicting the isobaric lines within the capillary for blood speeds 1 (Fig. 7a), 5 (Fig. 7b) and 10 mm/s (Fig. 7c). All cases are for a single RBC flowing through the capillary, i.e., for hematocrit equal to 3.09%.

From top to bottom, Fig. 7 reveals that increasing the blood speed results in the thinning of the boundary layer around the RBC. This means the RBC surface is exposed to a steeper CO partial-pressure gradient, with translates into more mass transfer to the RBC. Observe the thinning boundary layer effect happens all around the RBC, not only along the frontal RBC area.

Also, as the blood speed increases, the extent to which the capillary membrane is affected by changes in the partial-pressure of CO increases. That is, the capillary membrane surface area affected for blood speed equal to 10 mm/s, Fig. 7c, is greater than the surface area for blood speed equal to 1 mm/s, Fig. 7a. The isobaric lines in front of the RBCs (to the left) expand, while they shrink behind the RBC (to the left). As the blood speed increases, the expansion becomes more pronounced than the shrinkage, resulting on an increase in convective effects. To some extend, the shrinkage of the iso-lines in the back of the RBCs is also caused by the plasma replenishment, i.e., the incoming of fresh plasma into the capillary. This effect seems to diminish as the number of red cells within the capillary increases (higher hematocrit) due to the smaller entrance zone along the capillary and the overall smaller plasma volume.

Fig. 8a for parachute-shaped RBCs shows the lung diffusing capacity per RBC, as affected by increasing the number of RBCs and the blood speed. Observe that DL_{RBC} decreases with an increase in the number of RBCs flowing through the capillary. The blood speed effect is reduced as the number of RBCs increase due to the hindering of the circulation between the RBCs and the lessening of the plasma replenishing effect. For comparison purposes, Fig. 8b) for circular RBCs is included as well. Observe the blood speed effect predominates to a higher number of RBCs in the case of circular RBCs. This is clearly a consequence of the aerodynamics (shape) of the RBC: a circular shape affects less the circulating flow between RBCs as the number of RBCs increase.

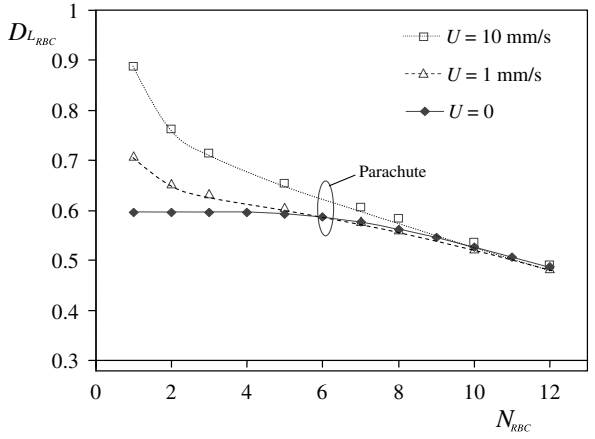

Fig. 8a. Variation of DL_{RBC} (capillary diffusing capacity per RBC) with number of RBCs for parachute-shaped RBCs.

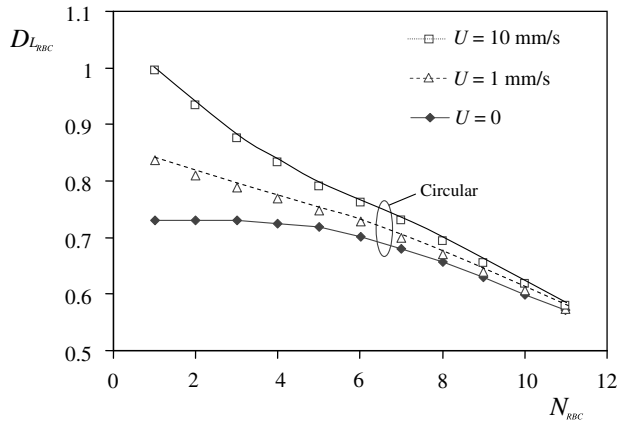

Fig. 8b. Variation of DL_{RBC} (capillary diffusing capacity per RBC) with number of RBCs for circular RBCs (from [12]).

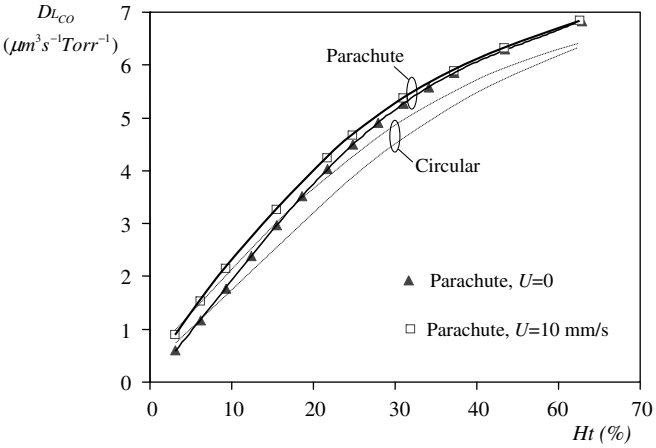

Fig. 9. Variation of capillary DL_{CO} with Ht for circular and parachute-shaped RBCs.

3.3. Convection dominance

Fig. 9 shows variation of capillary diffusing capacity with the capillary hematocrit, Ht:

$$\mathrm{Ht} = \frac{V_{\mathrm{RBC}} N_{\mathrm{RBC}}}{V_{\mathrm{cap}}} \tag{13}$$

for blood speed 0 and 10 mm/s. It is evident that convection is dominant when the hematocrit is small (i.e., for less number of red cells in the capillary), with the diffusing capacity value approaching that for pure diffusion as the hematocrit increases. Again included in the same graph are results for circular RBCs from [12]. Observe the lung diffusing capacity of parachute-shaped RBCs is higher than of circular-shaped RBCs.

The effects of blood flow for parachute-shaped RBCs are summarized in Fig. 10, where ε, the relative percentage difference between the DL_d (for pure diffusion, no blood flow, with $\theta_{CO} \to \infty$) and the DL_c for convection (with blood flow), defined as

$$\varepsilon = \left| \frac{\mathrm{DL_c} - \mathrm{DL_d}}{\mathrm{DL_d}} \right| \times 100 \tag{14}$$

is shown for several hematocrit values, Ht. Two blood speeds are considered, namely $U = 1$ and 10 mm/s. The results indicate that the blood speed affects the lung diffusing capacity by 50% in some cases, the effect being more pronounced as the blood speed increases and the hematocrit decreases. Finally, the variation of ε with

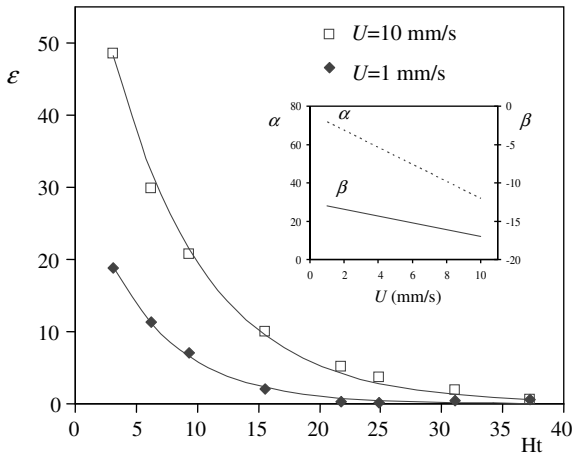

Fig. 10. Variation of ε with capillary Ht for parachute RBCs (for $\theta_{CO} \to \infty$).

Ht is captured through curve fitting the numerical results, yielding the following formula:

$$\varepsilon = \alpha e^{-(\beta Ht)} \tag{15}$$

for which values of α and β, arbitrary constants, are shown in Fig. 10 as well for different blood speeds.

4. Summary and conclusion

The effect of blood flow and RBC shape on the transport of CO in an alveolar capillary was investigated numerically. Parachute-shaped RBCs were modeled as moving (fluidized) particles, flowing with plasma in a pulmonary capillary.

The numerical simulation results yield 48% difference between DL_{CO} predicted for a blood speed of 10 mm/s and DL_{CO} predicted for stationary blood for the lowest hematocrit considered here (about 3%). This is comparable to the almost 60% difference predicted for circular RBC by Merrikh and Lage [12].

The present study compares also results for parachute-shaped RBCs to results for circular-shaped RBCs reported previously. It is found that circular-shaped RBCs are more efficient in up-taking CO on a per RBC basis. However, for the equivalent hematocrit, the parachute-shaped RBCs are shown to be more efficient. The difference between parachute and circular shapes is more pronounced at high capillary hematocrit (Ht > 40%).

The results obtained reveal that, in contrary to the seminal work of Aroesty and Gross [9], blood speed effects are significant in altering the diffusing process in alveolar capillary, especially at low hematocrit and high blood speed.

References

[1] A. Krogh, M. Krogh, Rate of diffusion into lungs of men, Skand. Arch. Physiol. 23 (1909) 236–247.
[2] American Thoracic Society, Single breath carbon monoxide diffusing capacity (transfer factor): recommendations for a standard technique, Am. J. Resp. Crit. Care Med. 152 (1995) 2185–2198.
[3] J.M.B. Hughes, D.V. Bates, Historical review: the carbon monoxide diffusing capacity (DL_{CO}) and its membrane (DM) and red cell (θV_C) components, Resp. Phys. Neurobiol. 138 (2003) 142–155.
[4] M. Krogh, The diffusion of gases through the lungs of man, J. Physiol. (London) 49 (1915) 271–296.
[5] J.H. Comroe, Jr., R.E. Forster, A.B. Dubois, W.A. Briscoe, E. Carlsen, The Lung: Clinical Physiology and Pulmonary Function Tests, second ed., Year Book Medical Publishers, Chicago, 1962 (reprint: 1974).
[6] F.J.W. Roughton, R.E. Forster, Relative importance of diffusion and chemical reaction rates in determining the rate of exchange of gases in human lung, with special reference to true diffusion capacity of the pulmonary membrane and volume of blood in lung capillaries, J. Appl. Physiol. 11 (1957) 290–302.
[7] R.L. Johnson Jr., H.F. Taylor, A.C. DeGraff, Functional significance of a low pulmonary diffusing capacity for carbon monoxide, J. Clin. Invest. 44 (1965) 789–800.
[8] E.R. Weibel, Morphometric estimation of pulmonary diffusion capacity I. Model and method, Resp. Physiol. 11 (1970) 54–75.
[9] J. Aroesty, J.F. Gross, Convection and diffusion in the microcirculation, Microvasc. Res. 2 (1970) 247–267.
[10] A.A. Merrikh, Convection–diffusion analysis of gas transport in a pulmonary capillary, Ph.D. thesis, Southern Methodist University, Dallas, TX, 2004.
[11] A.A. Merrikh, J.L. Lage, Effect of blood flow on gas transport in a pulmonary capillary, ASME J. Biomech. Eng. 127 (3) (2005) 432–439.
[12] A.A. Merrikh, J.L. Lage, The role of red cell movement on alveolar gas diffusion, J. Mater. Sci. Eng. Technol. 36 (10) (2005) 497–504.
[13] J.D. Hellums, The resistance to oxygen transport in the capillaries relative to that in the surrounding tissue, Microvasc. Res. 13 (1977) 131–136.
[14] W.J. Federspiel, A.S. Popel, A theoretical analysis of the effect of the particulate nature of blood on oxygen release in capillaries, Microvasc. Res. 32 (1986) 164–169.
[15] W.J. Federspiel, Pulmonary diffusing capacity: implications of two-phase blood flow in capillaries, Resp. Physiol. 77 (1989) 119–134.
[16] K. Groebe, G. Thews, Effect of red cell spacing and red cell movement upon oxygen release under conditions of maximally working skeletal muscle, Adv. Exp. Med. Biol. 248 (1989) 175–185.
[17] C.-H. Wang, A.S. Popel, Effect of red blood cell shape on oxygen transport in capillaries, Math. Biosci. 116 (1993) 89–110.
[18] C.C.W. Hsia, C.J.C. Chuong, R.L. Johnson Jr., Critique of conceptual basis of diffusion capacity estimates: a finite element analysis, J. Appl. Physiol. 79 (1995) 1039–1047.
[19] C.C.W. Hsia, C.J.C. Chuong, R.L. Johnson Jr., Red cell distortion and conceptual basis of diffusion capacity estimates: a finite element analysis, J. Appl. Physiol. 83 (1997) 1397–1404.
[20] A.O. Frank, C.J.C. Chuong, R.L. Johnson Jr., A finite element model of oxygen diffusion in the pulmonary capillaries, J. Appl. Physiol. 82 (1997) 2036–2044.
[21] C. Bos, L. Hoofd, T. Oostendorp, Reconsidering the effect of local plasma convection in a classical model of oxygen transport in capillaries, Microvasc. Res. 51 (1996) 39–50.
[22] S. Patel, Evaluation of the resistance of membrane and erythrocytes to oxygen transport in pulmonary capillaries, Resp. Physiol. Neorobiol. 130 (2002) 181–187.
[23] R. Skalak, P.I. Branemark, Deformation of red blood cells in capillaries, Science 9 (1969) 717–719.